ISSN 1063-7397, Russian Microelectronics, 2017, Vol. 46, No. 3, pp. 216–223. © Pleiades Publishing, Ltd., 2017.
Original Russian Text © B.G. Konoplev, E.A. Ryndin, M.A. Denisenko, 2017, published in Mikroelektronika, 2017, Vol. 46, No. 3, pp. 236–244.

Circuit Model for Functionally Integrated Injection Laser Modulators

B. G. Konoplev, E. A. Ryndin*, and M. A. Denisenko

Institute of Nanotechnology, Electronics, and Electronic Equipment Engineering, Southern Federal University, Taganrog, 347928 Russia

**e-mail: rynenator@gmail.com*

Received June 22, 2016

Abstract—This paper proposes a circuit model for injection lasers with functionally integrated optical-radiation modulators. This model takes into account the design and structural features of the functionally-integrated injection laser modulators (FIILMs), as well as the effect exerted by the spatial distributions of electrons, holes, and photons in the FIILMs' active region on the behavior of the physical processes there.

DOI: 10.1134/S1063739717030040

1. INTRODUCTION

The problem of interconnections in electronic equipment is one of the key problems for modern electronics. Traditional metal interconnections, in certain cases, fail to meet the stricter requirements for transmission quality, speed, and noise immunity. This problem takes place at all structural levels of electronic equipment, including interconnections in integrated circuits. One of the promising methods for solving this problem in microelectronics is the use of integrated optical switching systems and the corresponding optoelectronic components, the most important of which are integrated injection lasers and optical-radiation modulators.

In [1–5], high-speed laser modulators were described that functionally integrate an injection laser with an optical-radiation modulator to form a consistent nano-heterostructure, which implements amplitude [1] or frequency [2, 3] modulation, depending on the structure of the active region. The research and development of these functionally-integrated injection laser modulators (FIILMs) calls for new physical and topological models (e.g., in the form of systems of partial differential equations), as well as more compact circuit models (which would allow us to significantly reduce the time and computational costs of simulation). These compact circuit models can be constructed using commercial software (for example, SPICE).

The purpose of this work is to develop a circuit model for amplitude-modulated optical radiation FIILMs.

2. OPERATING PRINCIPLE OF THE FUNCTIONALLY INTEGRATED INJECTION LASER MODULATOR

A FIILM is a semiconductor nano-heterostructure that functionally integrates the highly-alloyed $p+$ and $n+$ regions with ohmic (supply) contacts and the modulator regions with additional (control) contacts and control junctions (Schottky junction and p-n junction) to form a quantum well system of a certain configuration [1, 4, 5]. The band diagrams in Fig. 1 schematically show that the heterostructure of a FIILM's active region contains two spatially displaced but equally widened potential wells: the first one in the conduction band and the second one in the valance band.

In a FIILM supply circuit, a certain pumping value is set to ensure (upon completion of the transport process) the inverse population of the potential wells and the time-constant total number of electrons and holes in them. The amplitude of the optical radiation is modulated by changing the direction of the transverse control field (see Fig. 1). One direction of the control field leads to the relocation and spatial superposition of the peak densities of the electrons and holes in the potential wells of the conduction and valance bands (which increases the optical radiation intensity), while the opposite direction leads to the reverse relocation and, therefore, spatial separation of the peak densities (which decreases the optical radiation intensity).

If the level of the electrons and holes injected into the FIILM active region is constant, then (when changing the direction of the transverse control field) the total number of charge carriers in the quantum wells remains almost the same. In this case, the maximum modulation frequency of a laser beam depends on the controlled relocation of the peak densities of

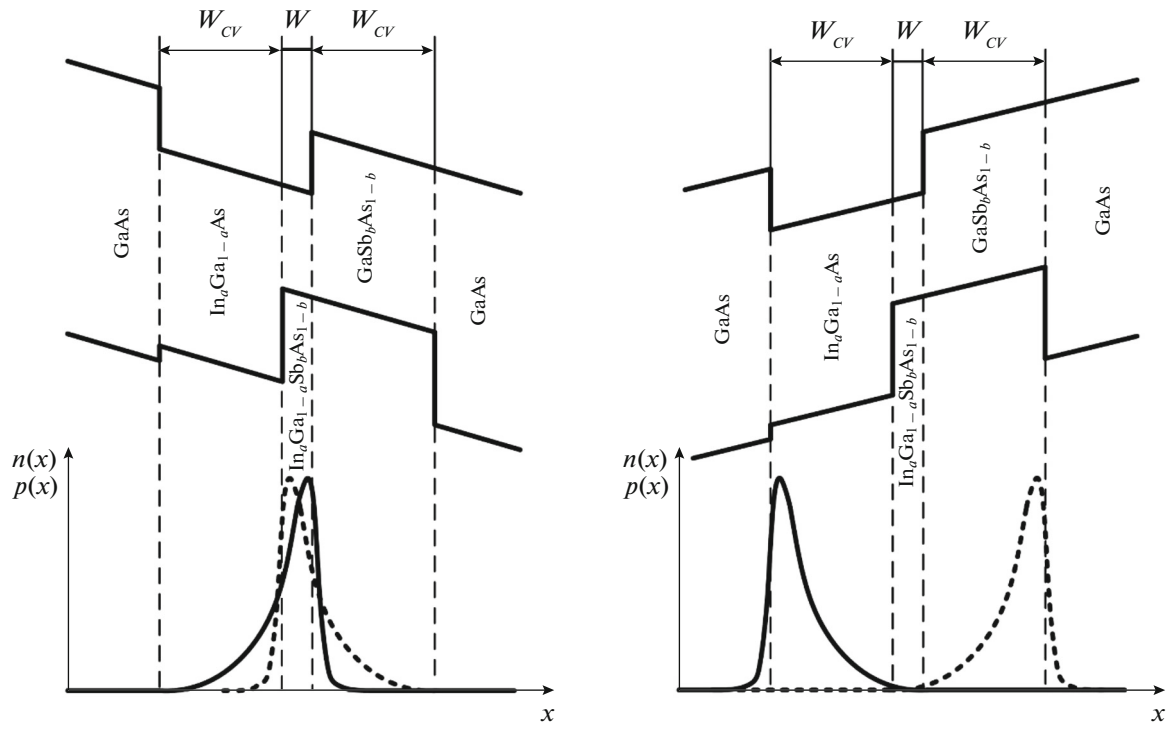

Fig. 1. Band diagrams and concentrations of electrons ($n(x)$, shown by solid lines) and holes ($p(x)$, shown by dashed lines) in FIILM for opposite directions of control field [6].

the electrons and holes in the spatially displaced potential wells rather than on the relatively inertial processes of carrier accumulation and escape [1, 4].

Taking this into account, the effectiveness of the FIILM design methods [6] can be improved by developing new physical and topological models (in the form of systems of partial differential equations [7, 8]), as well as more compact circuit models (which can be constructed using commercial software, e.g., SPICE).

3. FIILM CIRCUIT MODEL

The circuit model that describes the behavior of the physical processes taking place in a FIILM is developed based on the considerations and assumptions presented below. However, first, let us introduce some designations. We denote the width of the potential wells' spatial intersection region by W and the width of the potential wells' spatial displacement region by W_{CV} (Fig. 1). According to the electroneutrality principle, the electron and hole concentrations averaged over the volume of the W-wide potential wells' spatial intersection region are equal. These averaged concentrations are denoted by n.

Taking into account the specific characteristics of the heterostructure shown in Fig. 1 (see [5]), the electron concentration averaged over the volume of the W_{CV}-wide potential wells' spatial displacement region in the conduction band will exceed by several orders the similarly averaged hole concentration, while the hole concentration averaged over the volume of the corresponding region in the valance band will exceed by several orders the similarly averaged electron concentration. Moreover, taking into account both the equal widths of the potential wells and the electroneutrality principle, the electron concentration averaged over the potential wells' spatial displacement region in the conduction band can be regarded as equal to the similarly averaged hole concentration in the valance band. These averaged carrier concentrations are denoted by n_{CV}.

Taking into account the FIILM's operating principles considered above, the rates of time t variations in the carrier concentrations averaged over the wells' spatial intersection and spatial displacement regions $\frac{dn}{dt}$ and $\frac{dn_{CV}}{dt}$ can be represented as the sums of two components. The components of the first sum, $\left.\frac{dn}{dt}\right|_{\|}$ and $\left.\frac{dn_{CV}}{dt}\right|_{\|}$, are due to the injection of electrons and holes from the highly alloyed supply contact regions under the action of both the pumping current and the longitudinal component of the electric field. In turn, the components of the second sum, $\left.\frac{dn}{dt}\right|_{\perp}$ and $\left.\frac{dn_{CV}}{dt}\right|_{\perp}$, are

due to the relocation of the electrons and holes under the action of the transverse component of the control contact field. Thus, we have

$$\frac{dn}{dt} = \left.\frac{dn}{dt}\right|_{\parallel} + \left.\frac{dn}{dt}\right|_{\perp}; \quad (1)$$

$$\frac{dn_{CV}}{dt} = \left.\frac{dn_{CV}}{dt}\right|_{\parallel} + \left.\frac{dn_{CV}}{dt}\right|_{\perp}. \quad (2)$$

The component $\left.\frac{dn}{dt}\right|_{\parallel}$ depends not only on the pumping current $j(t)$ but also on the processes of radiative recombination (spontaneous and stimulated):

$$\left.\frac{dn}{dt}\right|_{\parallel} = \frac{j(t)}{eL} - \frac{n}{\tau_S} - v_g n_{ph} g(n, n_{ph}); \quad (3)$$

$$v_g = \frac{c}{n_A}, \quad (4)$$

where n_{ph} is the photon density in the FIILM's active region, L is the length of the FIILM's active region (the distance between the boundaries of the highly alloyed $n+$ and $p+$ regions of the supply contacts), e is the elementary charge, v_g is the photon velocity in the active region, c is the speed of light in vacuum, n_A is the index of light refraction in the active region, τ_S is the spontaneous radiative recombination time, and $g(n, n_{ph})$ is the optical gain coefficient.

The component $\left.\frac{dn_{CV}}{dt}\right|_{\parallel}$ is determined similarly; however, it takes into account only the spontaneous radiative recombination (since the conditions for laser generation do not hold in the potential wells' spatial displacement regions of the FIILM's heterostructure):

$$\left.\frac{dn_{CV}}{dt}\right|_{\parallel} = \frac{j(t)}{eL} - \frac{n_{CV}}{\tau_S}. \quad (5)$$

Since the spatial relocation of the charge carriers under the action of the transverse component of the control contact field can take place only inside the potential wells, the corresponding components of the rates characterizing the time variations in the averaged carrier concentrations are related as follows:

$$W \left.\frac{dn}{dt}\right|_{\perp} = -W_{CV} \left.\frac{dn_{CV}}{dt}\right|_{\perp}. \quad (6)$$

The components $\left.\frac{dn}{dt}\right|_{\perp}$ and $\left.\frac{dn_{CV}}{dt}\right|_{\perp}$ depend on the drift and diffusion of the charge carriers:

$$\left.\frac{dn}{dt}\right|_{\perp} = \frac{(\mu_n + \mu_p)/2}{W}\left(\frac{n_{CV}W_{CV} + nW}{W_{CV} + W} E + \varphi_T \frac{n_{CV} - n}{(W_{CV} + W)/2}\right); \quad (7)$$

$$\left.\frac{dn_{CV}}{dt}\right|_{\perp} = -\frac{(\mu_n + \mu_p)/2}{W_{CV}}\left(\frac{n_{CV}W_{CV} + nW}{W_{CV} + W} E + \varphi_T \frac{n_{CV} - n}{(W_{CV} + W)/2}\right); \quad (8)$$

$$E = E_0 + \frac{U_G(t)}{W_G}; \quad (9)$$

$$W_G = W_{BH} + W_{BL} + 2W_{CV} + W, \quad (10)$$

where U_G is the control voltage (the one between the control contacts), E is the strength of the transverse component for the electric field in the FIILM's active region, E_0 is the strength of the transverse component for the built-in field, W_{BH} is the width of the barrier n-region for the Schottky control junction, W_{BL} is the width of the n-region for the control p-n junction, W_G is the distance between the metallurgical boundaries of the control junctions (Schottky junction and p-n junction), μ_n and μ_p are the mobilities of the electrons and holes (respectively) in the potential wells, and φ_T is the temperature potential.

By substituting (3)–(5) and (7)–(10) into (1) and (2), as well as taking into account the kinetics equation for photon density [9], we obtain the FIILM model in the form of the differential equation system:

$$\begin{aligned}\frac{dn}{dt} &= \frac{j(t)}{eL} - \frac{n}{\tau_S} - v_g n_{ph} g(n, n_{ph}) \\ &+ \frac{1}{2W}\frac{\mu_n + \mu_p}{W_{CV} + W}\left[(n_{CV}W_{CV} + nW)\left(E_0 + \frac{U_G(t)}{W_G}\right) + 2\varphi_T (n_{CV} - n)\right];\end{aligned} \quad (11)$$

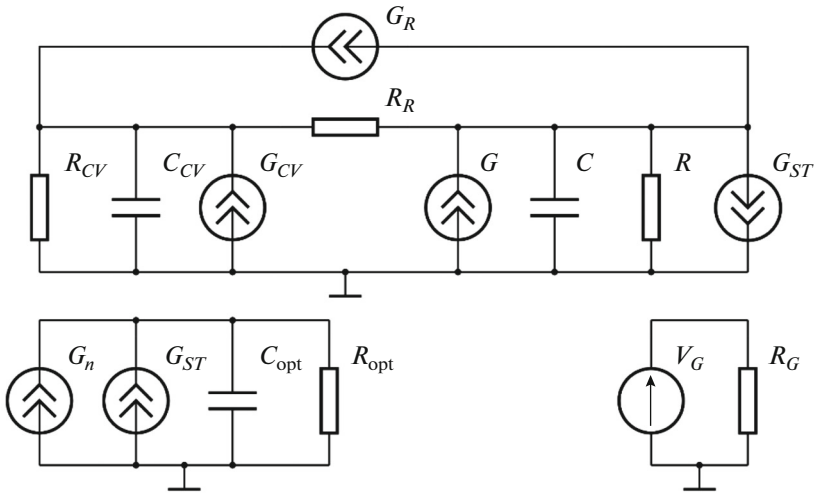

Fig. 2. FIILM equivalent circuit.

$$\frac{dn_{CV}}{dt} = \frac{j(t)}{eL} - \frac{n_{CV}}{\tau_S} - \frac{1}{2W_{CV}}\frac{\mu_n + \mu_p}{W_{CV} + W}\left[\left(n_{CV}W_{CV} + nW\right)\left(E_0 + \frac{U_G(t)}{W_G}\right) + 2\varphi_T\left(n_{CV} - n\right)\right]; \quad (12)$$

$$\frac{dn_{ph}}{dt} = -\frac{n_{ph}}{\tau_f} + \beta\frac{n}{\tau_S} + v_g n_{ph} g\left(n, n_{ph}\right), \quad (13)$$

where τ_f is the photon lifetime in the FIILM resonator and β is the portion of spontaneous optical radiation falling within the laser mode. The optical gain coefficient $g(n, n_{ph})$ is determined by the expressions presented in [10].

Upon integrating Eqs. (11) and (13) over the volume of the potential wells' spatial intersection region and integrating Eq. (12) over the volume of the potential wells' spatial displacement regions, we obtain the equations representable in the form of the equivalent circuit shown in Fig. 2.

In this equivalent circuit, the current sources G and G_{CV} determine the amounts of the pumping currents $I(t)$ to flow through the W-wide spatial intersection region and the W_{CV}-wide spatial displacement region, respectively:

$$G = \frac{W}{(W_{CV} + W)} I(t); \quad (14)$$

$$G_{CV} = \frac{W_{CV}}{(W_{CV} + W)} I(t). \quad (15)$$

The capacitances C and C_{CV} govern the charge accumulation processes in the regions of spatial intersection and spatial displacement, respectively; these capacitances are given by the expressions

$$C = C_0 L_R W; \quad (16)$$

$$C_{CV} = C_0 L_R W_{CV}, \quad (17)$$

where C_0 is the specific capacity of the injector junction and L_R is the distance between the cavity mirrors.

The resistances R and R_{CV} determine the spontaneous radiative recombination rates in the regions of spatial intersection and spatial displacement, respectively; these resistances are given by the expressions

$$R = \frac{\tau_S}{C_0 L_R W}; \quad (18)$$

$$R_{CV} = \frac{\tau_S}{C_0 L_R W_{CV}}. \quad (19)$$

The voltage-controlled current source G_{ST} determines the stimulated radiative recombination rate and, thereby, the stimulated photon generation rate in the spatial intersection region; this source is given by the expression

$$G_{ST} = \frac{\tau_f}{R_{\text{opt}}} v_g U_{\text{opt}} g\left(U, U_{\text{opt}}\right), \quad (20)$$

where U is the electric potential difference on the equivalent capacitance C (which characterizes the charge accumulated in the spatial intersection region), U_{opt} is the electric potential difference on the equivalent capacitance C_{opt} (which governs the photon accumulation in the FIILM's active region), and R_{opt} is the

resistance that governs the photon leakage from the resonator.

The elements C_{opt} and R_{opt} depend on the photon lifetime in the FIILM resonator:

$$R_{opt}C_{opt} = \tau_f. \quad (21)$$

The optical gain $g(U, U_{opt})$ in Eq. (20) is found by the formula

$$g(U,U_{opt}) = \frac{g_0}{\sqrt{1+\varepsilon_E\Gamma\dfrac{U_{opt}\tau_f}{eR_{opt}LL_RW}}}\ln\left(\frac{A_1\dfrac{U(t)C}{eLL_RW}+A_2\left(\dfrac{U(t)C}{eLL_RW}\right)^2+A_3\left(\dfrac{U(t)C}{eLL_RW}\right)^3}{A_1n_0+A_2n_0^2+A_3n_0^3}\right), \quad (22)$$

where n_0 is the mobile carrier's concentration in the FIILM's active region for which the laser generation conditions hold; g_0 is the m^{-1}-dimensional proportionality coefficient; A_1, A_2, and A_3 are the coefficients of the trap, radiative, and Auger recombinations, respectively; Γ is the optical confinement factor; and ε_E is the coefficient representing the sum of the effects that reduce the optical gain.

The voltage-controlled current source G_n determines the rate of spontaneous photon generation in the potential wells' spatial intersection region and is given by the expression

$$G_n = \beta\frac{U}{R}. \quad (23)$$

The voltage-controlled current source G_R reflects the drift component of the carriers' transverse relocation in the FIILM's active region and is given by the expression

$$G_R = \frac{C_0L_R}{2}\frac{\mu_n+\mu_p}{W_{CV}+W}(W_{CV}U_{CV}(t)+WU(t))\left(E_0+\frac{U_G(t)}{W_G}\right). \quad (24)$$

The resistance R_R reflects the diffusion component of the carriers' transverse relocation in the FIILM's active region and is given by the expression

$$R_R = \frac{W_{CV}+W}{\varphi_TC_0L_R(\mu_n+\mu_p)}. \quad (25)$$

The elements V_G and R_G determine the leakage currents in the control circuit: the EMF source V_G depends on the control's potential difference, while the resistance R_G depends on the leakage resistance of the control circuit.

4. SIMULATION RESULTS

The simulation results, which were obtained using the developed FIILM circuit model, are presented in Figs. 3 and 4. The simulation was carried out with the following parameters: $L = 200$ nm, $W = 5$ nm, $W_{CV} = 20$ nm, $W_{BH} = 50$ nm, $W_{BL} = 30$ nm, $\beta = 10^{-4}$, $\tau_f = 5$ ps, and $\tau_S = 4$ ns. The strength of the built-in field's transverse component E_0 stimulated the relocation of the electrons and holes into the potential wells' spatial intersection region and enabled laser generation for the pumping current exceeding a certain threshold and for a zero voltage across the control electrodes. The optical radiation was modulated in two ways: by impulsively varying the pumping current for a zero control voltage ($U_G = 0$) and by feeding the blanking pulse of the control voltage for the constant pumping current exceeding the threshold.

The FIILM's active region needs to be long enough (the distance between the boundaries of the highly alloyed $n+$ and $p+$ regions of the supply contacts was $L = 200$ nm) to ensure the effectiveness of the optical radiation modulation by the transverse electric field of the control contacts. The strength of the built-in field's transverse component E_0 and the active region's length L were selected based on the results of the FIILM's numerical simulation using the physical and topological model considered in [9].

Figure 3 demonstrates the transport processes in the FIILM for the case of optical radiation modulation by the pumping current pulse (shown in Fig. 3a).

Figure 4 demonstrates the transport processes in the FIILM for the case of optical radiation modulation by the control voltage pulse (shown in Fig. 4a).

The modulation by the pumping current pulse (see Fig. 3b) simultaneously increased or decreased the carrier concentrations in the spatial intersection and spatial displacement regions of the heterostructure. In this case, the duration of the transport processes

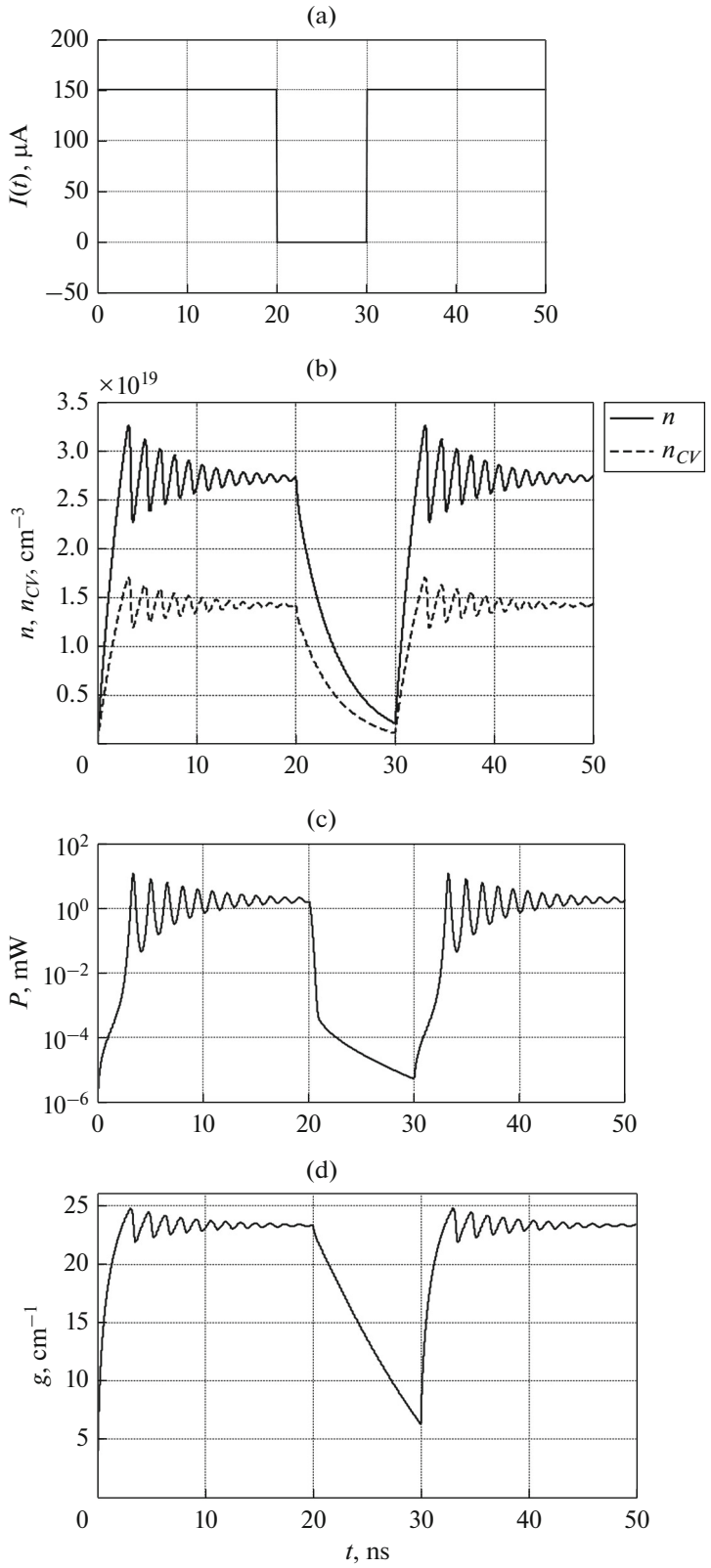

Fig. 3. (a) Transport processes in case of modulation by pumping current pulse, (b) carrier concentrations in spatial intersection n and spatial displacement n_{CV} regions, (c) optical radiation power, and (d) optical gain.

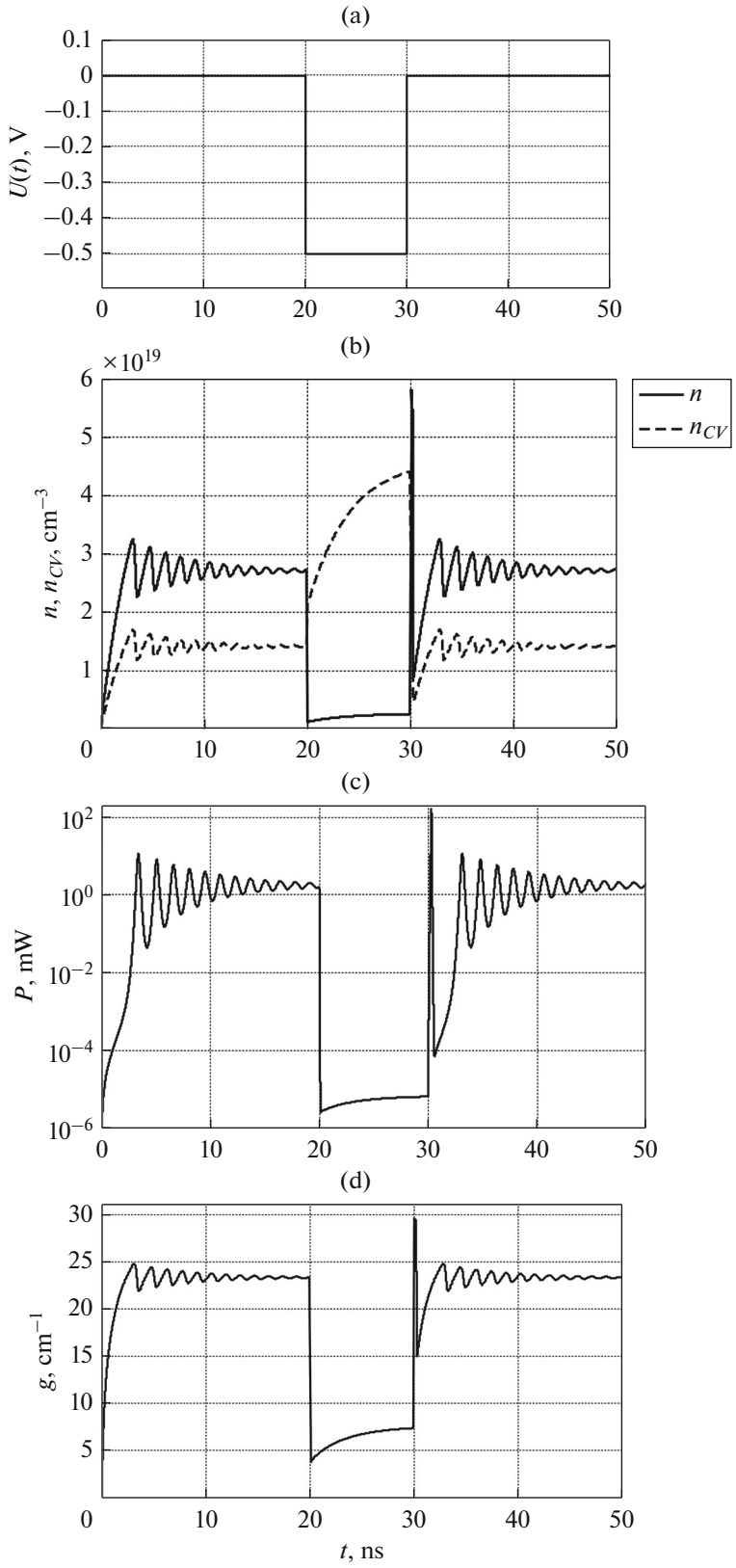

Fig. 4. (a) Transport processes in case of modulation by control voltage pulse, (b) carrier concentrations in spatial intersection n and spatial displacement n_{CV} regions, (c) optical radiation power, and (d) optical gain.

depended on the accumulation and escape rates of the electrons and holes in the FIILM's active region and amounted to tens of nanoseconds. The time dependence of the optical radiation power (Fig. 3c) shows that, in the case of modulation by the pumping pulse, the durations of the optical pulse edges exceeded 3.5 ns.

Figure 4b shows that, in the case of modulation by the control voltage $U_G(t)$ pulse, the carrier concentration n in the potential wells' spatial intersection region decreased with the simultaneous increase of the carrier densities n_{CV} in the spatial displacement regions (and vice versa, n increased with decreasing n_{CV}); this indicates the spatial relocation of the peak carrier concentrations between these regions of the heterostructure. In the process of relocation, the total number of electrons and holes in the FIILM's active region changed slightly.

Thus, in the case of optical radiation modulation by the control voltage pulses for a constant pumping current, the duration of the transport processes depends mainly on the time required for the relocation of the peak carrier concentrations between the spatial intersection and spatial displacement regions rather than on the accumulation and escape rates of the electrons and holes in the FIILM's active region. The time dependence of the optical radiation power (Fig. 4c) shows that, in the case of modulation by the control voltage, the durations of the leading and trailing optical pulse edges were 250 ps and 70 ps (respectively), which is by factors ranging from 14 to 50 lower than in the case of modulation by the pumping current.

5. CONCLUSIONS

As a result of this investigation, a FIILM circuit model has been developed; a FIILM is a semiconductor nano-heterostructure that functionally integrates the highly alloyed $p+$ and $n+$ regions with ohmic (supply) contacts and the modulator regions with additional (control) contacts and control junctions (Schottky junction and p-n junction) to form a quantum well system of a certain configuration [1, 4, 5].

The transport processes in the FIILM were simulated, in the first case, by impulsively varying the pumping current for zero control voltage and, in the second case, by feeding the control voltage pulse for a constant pumping current.

The analysis of the simulation results has showed that, in the case of optical radiation modulation by the control voltage (for the constant pumping current), the durations of the optical pulse edges were by factor of 14 to 50 shorter than in the case of modulation by the pumping current.

This is explained by the fact that, for a constant pumping current (and, therefore, for a constant level of the electrons and holes injected into the FIILM's active region), the total number of charge carriers in the potential wells remains almost the same (when changing the direction of the transverse control field). Therefore, the durations of the optical pulse edges depend on the controlled relocation of the peak carrier concentrations in the spatially displaced potential wells of the FIILM's active region rather than on the relatively inertial processes of carrier accumulation and escape.

ACKNOWLEDGMENTS

The results were obtained on the equipment provided by the Research and Education Center and the Nanotekhnologii Center for Collective Use of the Institute of Nanotechnology, Electronics, and Electronic Equipment Engineering of the Southern Federal University (Taganrog).

This work was supported by the Russian Foundation for Basic Research (project no. 16-07-00018) and the Ministry of Education and Science of the Russian Federation (project no. 16.5981.2017/BCh).

REFERENCES

1. Konoplev, B.G., Ryndin, E.A., and Denisenko, M.A., Integrated injection laser with rearrangement of wave functions of carriers, *Vestn. Yuzh. Nauch. Tsentra RAN,* 2010, vol. 6, no. 3, pp. 5–11.
2. Ryndin, E.A. and Denisenko, M.A., A functionally integrated injection laser-modulator with the radiation frequency modulation, *Russ. Microelectron.,* 2013, vol. 42, no. 6, pp. 360–362.
3. Konoplev, B.G., Ryndin, E.A., and Denisenko, M.A., Injection laser with a functionally integrated frequency modulator based on spatially shifted quantum wells, *Tech. Phys. Lett.,* 2013, vol. 39, no. 11, pp. 986–989.
4. Konoplev, B.G., Ryndin, E.A., and Denisenko, M.A., Components of integrated microwave circuits based on complementary coupled quantum regions, *Russ. Microelectron.,* 2015, vol. 44, no. 3, pp. 190–196.
5. Konoplev, B.G., Ryndin, E.A., and Denisenko, M.A., Integrated injection laser with rearrangement of wave functions of carriers, RF Patent no. 2400000, 2010.
6. Ryndin, E.A. and Denisenko, M.A., The method of functionally integrated laser-modulators design, *Inzh. Vestn. Dona,* 2013, no. 3, pp. 1–6.
7. Konoplev, B.G. and Ryndin, E.A., A study of the transport of charge carriers in coupled quantum regions, *Semiconductors,* 2008, vol. 42, no. 13, pp. 1462–1468.
8. Ryndin, E.A. and Denisenko, M.A., Model of fuctional-integrated injected laser-modulators for integrated optical switching systems, *Izv. Vyssh. Uchebn. Zaved., Elektron.,* 2012, no. 6 (98), pp. 26–35.
9. Konoplev, B.G., Ryndin, E.A., and Denisenko, M.A., Numerical modeling of functionally integrated injection lasers-modulators, *Proc. SPIE,* 2014, vol. 9440, p. 944014. doi 10.1117/12.2180082
10. Zarifkar, A., Ansari, L., and Moravvej-Farshi, M.K., An equivalent circuit model for analyzing separate confinement heterostructure quantum well laser diodes including chirp and carrier transport effects, *Fiber Integr. Opt.,* 2009, no. 28, pp. 249–267.

Translated by Yu. Kornienko